# Influence of the ventilation strategy on the respiratory droplets dispersion inside a coach bus: CFD approach



# Influence of the ventilation strategy on the respiratory droplets dispersion inside a coach bus: CFD approach

*Mauro* Scungio[1] , *Giulia* Parlani[1,*], *Giacomo* Falcucci[2, 3]

[1] Department of Economics, Engineering, Society and Business Organization (DEIM). University of Tuscia, Via del Paradiso 47, Viterbo, Italy.
[2] Dipartimento di Ingegneria dell'Impresa "Mario Lucertini" - Università di Roma "Tor Vergata", Via del Politecnico 1, 00133, Roma
[3] Dept. of Physics - Harvard university, 17 Oxford Street, 02138 Cambridge (MA), USA

**Abstract.** The airborne transmission of the COVID-19 virus was considered the main cause of infection. The increasing concern about the virus spread in confined spaces, characterized by high crowding indexes and an often-inadequate air exchange system, pushes the scientific community to the design of many studies aimed at improving indoor air quality. The risk of transmission depends on several factors such as droplet properties, virus characteristics, and indoor airflow patterns. The main transmission route of the SARS-CoV-2 virus to humans is the respiratory route through small (<100 µm) and large droplets. In an indoor environment, the air exchange plays a fundamental role on the dispersion of the droplets. In this study, an integrated approach was developed to evaluate the influence of the ventilation strategy on the dispersion of respiratory droplets emitted inside a coach bus. There are no specific guidelines and standards on the air exchange rate (AER) values to be respected in indoor environments such as coach buses. The aim of this work is to analyse the influence of ventilation strategy on the respiratory droplet concentration and distribution emitted in a coach bus. Ansys FLUENT was used to numerically solve the well-known transient Navier-Stokes equations (URANS equations), the energy equation and using the Lagrangian Discrete Phase Model (DPM) approach to construct the droplet trajectories. The geometry is representative of an intercity bus, a vehicle constructed exclusively for the carriage of seated passengers. The 3D CAD model represented a coach bus with an HVAC system, within which an infected subject was present. The positions of exhaust vents and air-conditioning vents were chosen to ensure complete air circulation throughout the bus. The infected subject emitted droplets with a well-defined size distribution and mass through the mouth. The air exchange is provided in two different ways: general ventilation (from air intakes positioned along the bus windows and top side of central corridor) and personal ventilation (with air intakes for each passenger). For the general ventilation a single AER value was set (0.3 $m^3$ $s^{-1}$). The first results obtained showed a slight particle dispersion in the computational domain due to the airflow rate entered through the HVAC system, but a still elevated level of particle concentration tended to accumulate on the area near to infected subject. Additional analysis was executed to evaluate the beneficial effects linked to further addition of airflow through personal air-conditioning vents placed above every passenger's head. The results show the importance of the use of the ventilation system inside a coach bus, highlighting how the contribution linked to of the personal air exchange rate can lead to a significant reduction of droplet concentration exposure and consequently a reduction of the risk of infection from airborne diseases.

*Corresponding author: giulia.parlani@unitus.it

## 1. Introduction

The SARS-CoV-2 pandemic dictated the need for investigating the potential transmission scenario of the SARS-CoV-2 virus. The transmission risk depends on various factors: droplet properties, indoor airflow patterns, and virus characteristics. Recent evidence has demonstrated that viruses are released during exhalation, talking, and coughing in microdroplets small enough (<100 μm in diameter) to remain suspended in air for long time [1]. The engineering studies have also indicated that an adequate ventilation system is mandatory to reduce the infection risk in confined spaces, especially in public transportations, offices, and stores. It is therefore essential to investigate as an increase in air-conditioning flow in an indoor environment favours the reduction of contaminated particles concentration. Experimental studies allowed to define the droplet characteristics exhaled during respiratory activities (oral breathing and speaking) in terms of size and volume distributions (pre-and post-evaporation) and the distance travelled by airborne virus-laden particles [1, 2]. The information obtained is the results of airborne samples collected in indoor environments such as hospitals [3].
In indoor environments, using the ventilation system to minimise particle concentration is related to the impossibility of guaranteeing the minimum interpersonal distance [4]. Experimental studies on droplet analysis are complex and expensive; in addition, technological limits in terms of accuracy and functionality of devices limit the detection of all size ranges of particles. The progress of numerical modelling using Computational Fluid Dynamics (CFD) is a valuable support tool for research. CFD studies can provide detailed information in the time and space of thousands of airborne droplets by solving the mass, momentum and energy conservation equations and defining boundary conditions and appropriately turbulence model. In this case, the particles are the consequences of respiratory events that evaporate, collide, or separate due to thermal effects typical of indoor environments such as temperature, humidity, and air velocity.
In this work CFD simulations were carried out, using Ansys Fluent, in order to analyse the interactions between fluid and solid particles and evaluate the effect of different ventilation strategies on the respiratory droplets concentration and distribution inside a coach bus. The Discrete Phase Model (DPM) was used to solve the particle motion through the Eulerian-Lagrangian approach in a 3D model of coach bus provided with an HVAC system, within which an infected subject was present. The general ventilation system was considered to be always working, and then the effects linked to further addition of airflow through personal air-conditioning vents was analysed.
The results of the simulations allowed to describe the different spatial distributions of the respiratory droplets inside the bus considering different air exchange rates. In particular, the contribution to the dispersion of droplets due to the presence of personal air-conditioning vents was analysed.

## 2. Materials and methods

### *2.1. Mathematical model description*

Numerical simulations were conducted using the Ansys Fluent CFD software. This paper describes the diffusion process of particles in the air emitted by an infected passenger inside a coach bus. In this case, the Discrete Phase Model (DPM) allowed to describe the interaction of the continuous and discrete phases. The DPM regards fluid as a continuous phase and particles as a discrete phase and the two phases are coupled to each other [1].
The continuous phase is solved using Navier-Stokes equations while the discrete phase exchanges heat, momentum, mass, and energy with the continuous phase [1]. The DPM calculates the trajectory of each droplet by solving the individual droplet movement equation whose theory is Newton's second law:

$$m_{pt}\frac{d\boldsymbol{u}_{pt}}{dt} = \sum \boldsymbol{F}_D + \boldsymbol{F}_g \quad (1)$$

$$\frac{d\boldsymbol{x}_{pt}}{dt} = \boldsymbol{u}_{pt} \quad (2)$$

where $m_{pt}\ (kg)$ is the mass of the particle, $\boldsymbol{u}_{pt}\left(\frac{m}{s}\right)$ represents the particle velocity, $t\ (s)$ is the time, $\boldsymbol{F}_D\ (N)$ and $\boldsymbol{F}_g(N)$ are drag and gravity forces acting on the particle, $\boldsymbol{x}_{pt}\ (m)$ represents the trajectory of the particle. The drag force is given by:

$$\boldsymbol{F}_D = m_{pt}\frac{18}{\rho_{pt}\cdot d_{pt}^2}C_D\ \frac{Re_{pt}(\boldsymbol{u}_{air}-\boldsymbol{u}_{pt})}{24} \quad (3)$$

where $\rho_{pt}\left(\frac{kg}{m^3}\right)$, $d_{pt}(m)$ and $Re_{pt}$ represent respectively, the density, diameter, and Reynolds number of the particle. The particle density was constant and equal to 1200 kg m$^{-3}$. The $Re_{pt}$ was calculated as [2]:

$$Re_{pt} = \frac{\rho_{air}(|\boldsymbol{u}_{air}-\boldsymbol{u}_{pt}|)d_{pt}}{\mu} \quad (4)$$

The turbulence is modelled by the *Standard k-ε* model with Standard Wall Functions. The *k-ε* is a two-equation model that gives a general description of turbulence using two transport equations, the first variable is the turbulent kinetic energy (*k*), and the second transported variable is the rate of dissipation of turbulent kinetic energy (*ε*). The system of equations was discretized using the *SIMPLE* algorithm. In this study, the second-order discretization was chosen which allows for obtaining better results according to the geometric characteristics of the model.

*2.2. Droplet emissions*

Particle emission from the infected subject was modelled as a function of the breathing activity. A sinusoidal approximation of breathing activity was adopted considering the volumetric flow rate equal to 0.45 L s$^{-1}$ for mouth breathing [5]. Experimental analyses have shown that the size distribution of the emitted droplets falls in the range 0.5-1000 μm [3, 4] in the close proximity of the mouth of an adult person while breathing and speaking. These measurements are extremely complex due to the evaporation phenomenon typical of the respiratory particles as soon as they are emitted. The particles evaporation process reduces the particle diameter to about 20% of the emitted size [5].

For this reason, the post-evaporation number and volume distributions were considered in the CFD model and the five size ranges chosen in the simulation are related to the airborne respiratory particle range. Droplet diameter and droplets number and volume distribution are summarized in Table 1.

**Table 1.** Particle number (dN/dlog($d_{pt}$)) and volume (dV/dlog($d_{pt}$)) distributions (fitted by five size ranges) adopted in the simulations for breathing activities.

| **Particle diameter (size range), $d_{pt}$ (μm)** | **dN/dlog($d_{pt}$) (part. cm$^{-3}$)** | **dV/dlog($d_{pt}$) (μL cm$^{-3}$)** |
|---|---|---|
| 0.52 μm (<0.7 μm) | 0.312 | $2.33\times10^{-11}$ |
| 0.89 μm (0.7 to 1.2 μm) | 0.016 | $5.80\times10^{-12}$ |
| 1.53 μm (1.2 to 2.0 μm) | 0.005 | $1.03\times10^{-11}$ |
| 3.44 μm (2.0 to 5.9 μm) | 0.001 | $2.15\times10^{-11}$ |
| 7.71 μm (5.9 to 10.1 μm) | <0.001 | $3.44\times10^{-15}$ |

*2.3. Geometry, mesh, and boundary conditions*

Two domains were realized for the study. The first domain (D1, Figure 1) consisting of the whole coach bus was considered to evaluate the general droplet dispersion pattern. The second domain (D2, Figure 3) consisting in a section of the bus, was realized to simulate different personal air exchange rates and analyze the influence of the personal ventilation on the droplet dispersion.

The sizes of the domain D1, with a total internal volume of 47.88 m$^3$, refer to those of a long-distance bus, usually named intercity bus, a vehicle constructed exclusively for the carriage of seated passengers.

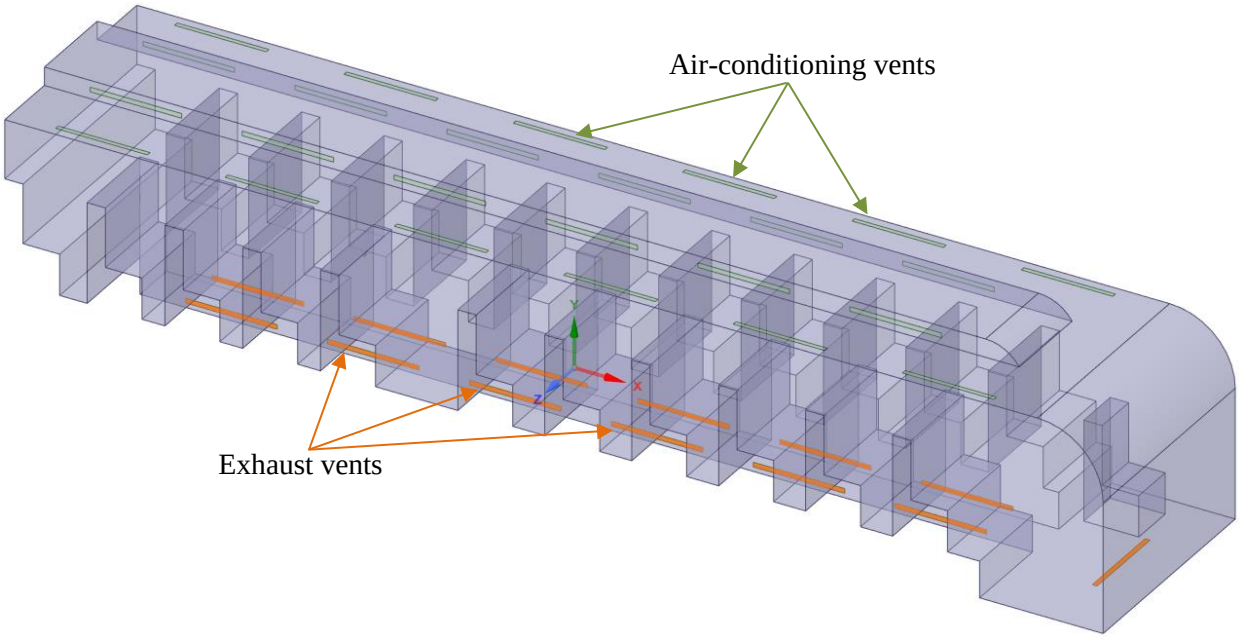


**Figure 1.** The computational domain (D1).

The coach bus consists of thirteen exhaust (orange box in Figure 1) vents on the lower part and twenty-four air-conditioning vents (green box in Figure 1) on the upper part of the bus. The mouth is outlined as a rectangular surface.
The efficiency of the HVAC system depends on the location of the diffuser and outlet and the flow rate of renewal air. The placement of outlet and air inlet vents must ensure the complete recirculating air. In particular, the air vents were designed so that to have a main airflow structure, from top to bottom of the bus to facilitate the dispersion of the emitted droplets. The airflow direction from air-conditioning vents and the gravity fosters the spread droplets downwards.
The contribution of the airflow was considered in terms of general and personal AER. While different studies have repeatedly emphasized as ventilation conditions significantly influence aerosol transport and deposition, there are no standards on the air exchange rate (AER) values to be respected in public transport [6].
In the first analysis, on the D1 domain, a single AER value was considered (0.3 $m^3 s^{-1}$) with air entering from the general air conditioning vents, without considering the personal ventilation. The infected subject emitted droplets with a well-defined size distribution and mass through the mouth modelled as a surface. A *user-defined function* (*UDF*) was used as boundary condition for the mouth of the infected subject to define the transient velocity profile through a sinusoidal function that describes the breathing activity.
A summary of all the input parameters used for the computational study is set out in Table 2 below.

**Table 2.** Boundary conditions of the D1 domain.

| Boundary Name | Boundary Condition | Boundary Condition Value | Lagrangian |
|---|---|---|---|
| Air-conditioning vents | Mass flow inlet | T = 298 K, Q = 0.3 $m^3 s^{-1}$ | escape |
| Mouth (Infected Subject) | Velocity Inlet | UDF, T = 310 K | escape |
| Exhaust vents | Pressure Outlet | 0 Pa | escape |
| Bus | Wall | Standard Wall Function, no-slip wall | escape |

The *hybrid initialization* allowed to set initial values for the flow variables and initialize the solution using these values. The D1 domain is discretized using a polyhedral grid with a total number of 2568154 nodes, as shown in Figure 2.

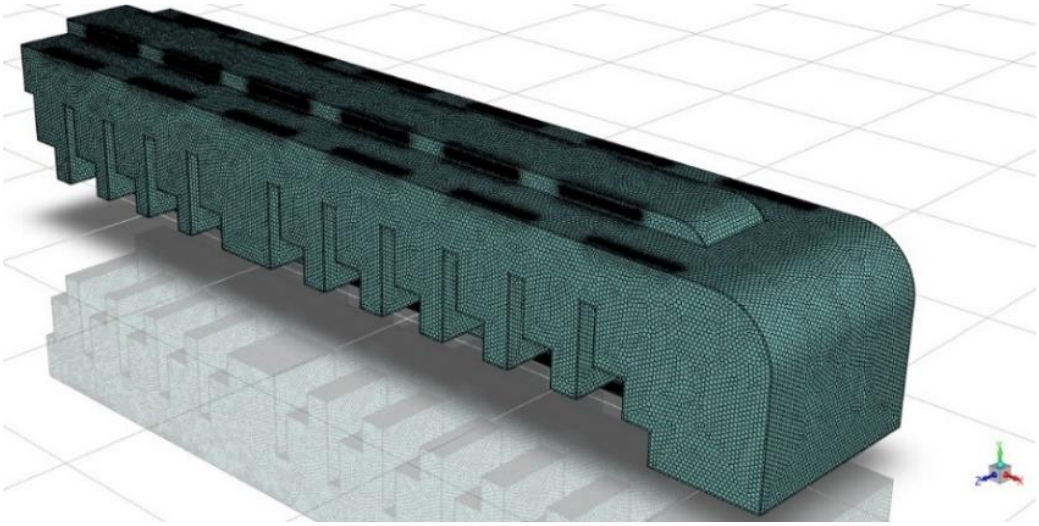

**Figure 2.** Grid of the D1 domain.

The personal conditioning vents provided in the D2 domain have a dimension of 4 cm x 3 cm and are located near each seat over every passenger's head. The D2 domain, representing a section of the bus, with the infected subject and the personal air-conditioning vents is reported in Figure 3.

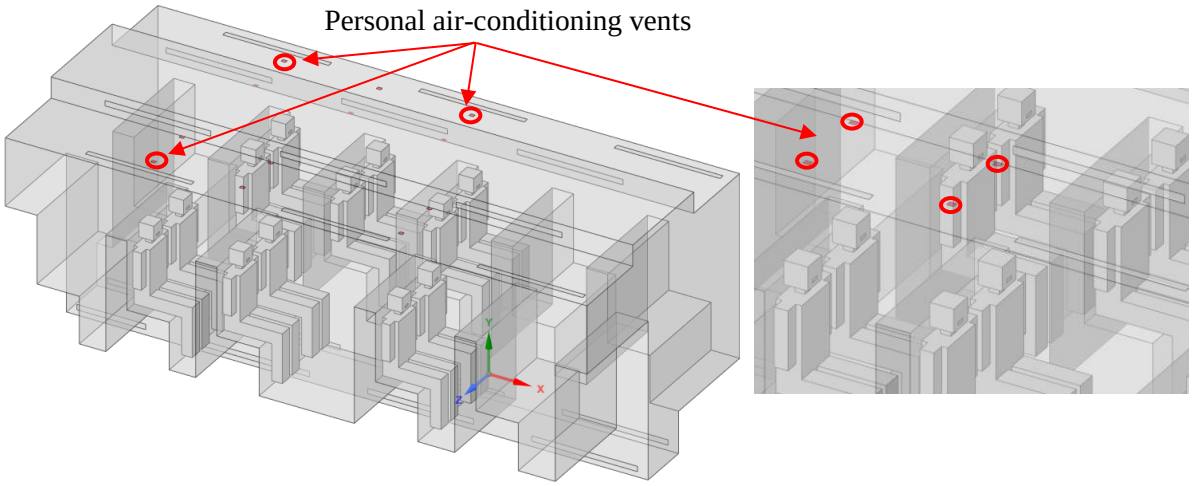


**Figure 3**: The D2 domain - Part of the bus.

The different values of air flows rate provided by the personal air conditioning vents, defined as personal AER, are summarized in Table 3.

**Table 3**. Personal air-conditioning vents – Personal AER values.

| AER [$h^{-1}$] | Mass flow rate [kg $s^{-1}$] |
|---|---|
| 1 | 0.0163 |
| 3 | 0.0489 |
| 5 | 0.0815 |
| 7 | 0.1141 |

The boundary conditions imposed are the same as in the earlier case except for the addition of the boundary condition of the *mass flow inlet* on the personal air-conditioning vents. A summary of input parameters used in the computational study is shown in Table 4.

**Table 4.** Boundary conditions of the D2 domain.

| Boundary Name | Boundary Condition | Boundary Condition Value | Lagrangian |
|---|---|---|---|
| Air-conditioning vents | Mass flow inlet | T = 298 K, Q = 0.3 $m^3$ $s^{-1}$ | escape |
| Personal air-conditioning vents | Mass flow inlet | T = 298 K, Q = refer to Table 3 | escape |
| Mouth (Infected Subject) | Velocity Inlet | UDF, T = 310 K | escape |
| Exhaust vents | Pressure Outlet | 0 Pa | escape |
| Bus | Wall | Standard Wall Function, no-slip wall | escape |

## 3. Results and discussion

A first CFD simulation was carried in order give a "first-attempt" estimation of the droplet distribution inside the whole bus model using the D1 domain. In this case a single AER value was considered (0.3 $m^3$ $s^{-1}$) with air entering from the general air conditioning vents, without considering the personal ventilation.

Figure 4 shows the time-evolution of droplet distribution inside the D1 domain from 30 s to 1800 s, while Figure 5 reports the time series of the droplet mass concentration for each droplet size in the same time period.

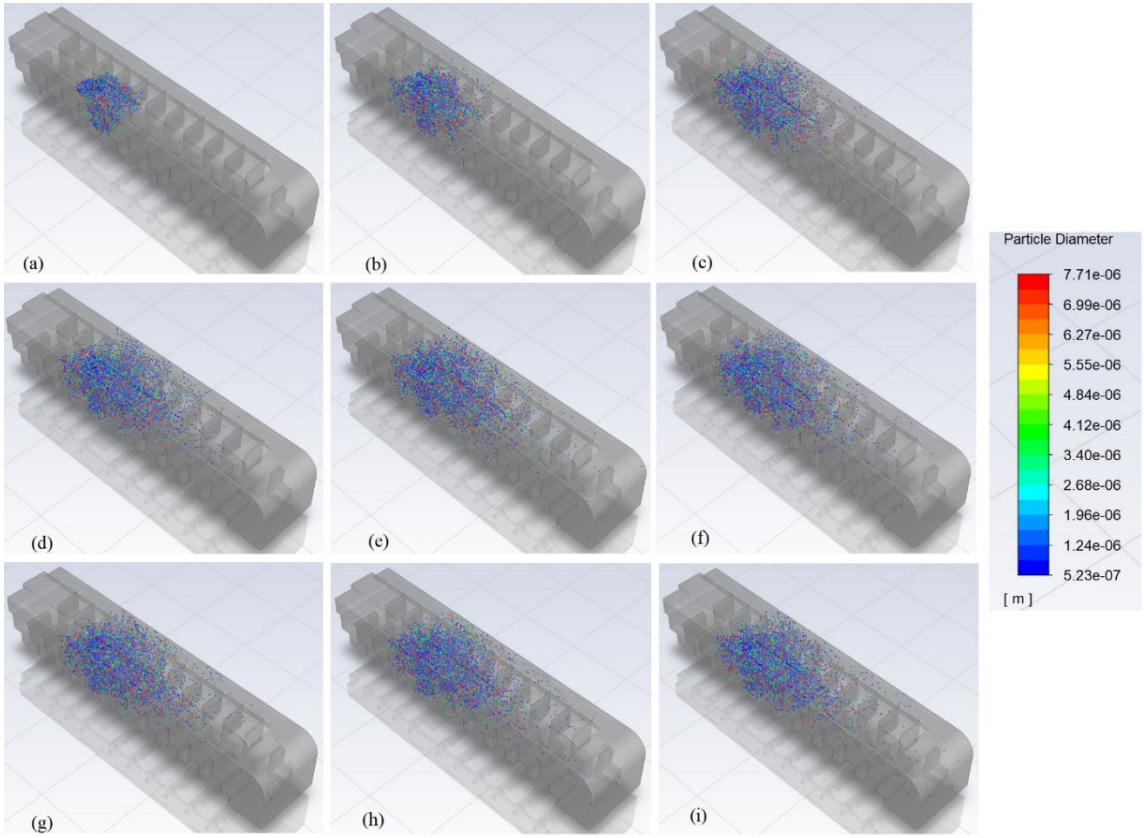


**Figure 4**. Spatial distribution of droplets inside the domain D1 for different diameters and for different times of the simulation: after 30 s (a); after 60 s (b); after 120 s (c); after 300 s (d); after 600 s (e); after 900 s (f); after 1200 s (g); after 1500 s (h); after 1800 s (i). The total droplet concentration inside the domain is $1.08\times10^{-4}$ µg/$m^3$ at 30 s (a); $1.67\times10^{-4}$ µg/$m^3$ at 60 s (b); $2.37\times10^{-4}$ µg/$m^3$ at 120 s (c); $2.80\times10^{-4}$ µg/$m^3$ at 300 s (d); $2.80\times10^{-4}$ µg/$m^3$ at 600 s (e); $2.75\times10^{-4}$ µg/$m^3$ at 900 s (f); $2.79\times10^{-4}$ µg/$m^3$ at 1200 s (g); $2.85\times10^{-4}$ µg/$m^3$ at 1500 s (h); $2.69\times10^{-4}$ µg/$m^3$ at 1800 s (i).

Looking at Figure 4 and Figure 5, the following points can be depicted: (i) the emitted droplets tend to concentrate close to the emitter, with a significant tendency to move in forward direction instead of moving backwards, along the bus; (ii) the droplet mass concentration becomes constant after 200 s of

simulation; (iii) the time series of droplet mass concentration show the same pattern for all the considered diameters. These general points lead to the conclusion that for the analysis of the impact of personal ventilation on the droplet distribution and dispersion patterns inside the coach bus, it could be sufficient to simulate only a section of the domain (domain D2), and considering a time interval of 900 s instead of 1800 s.

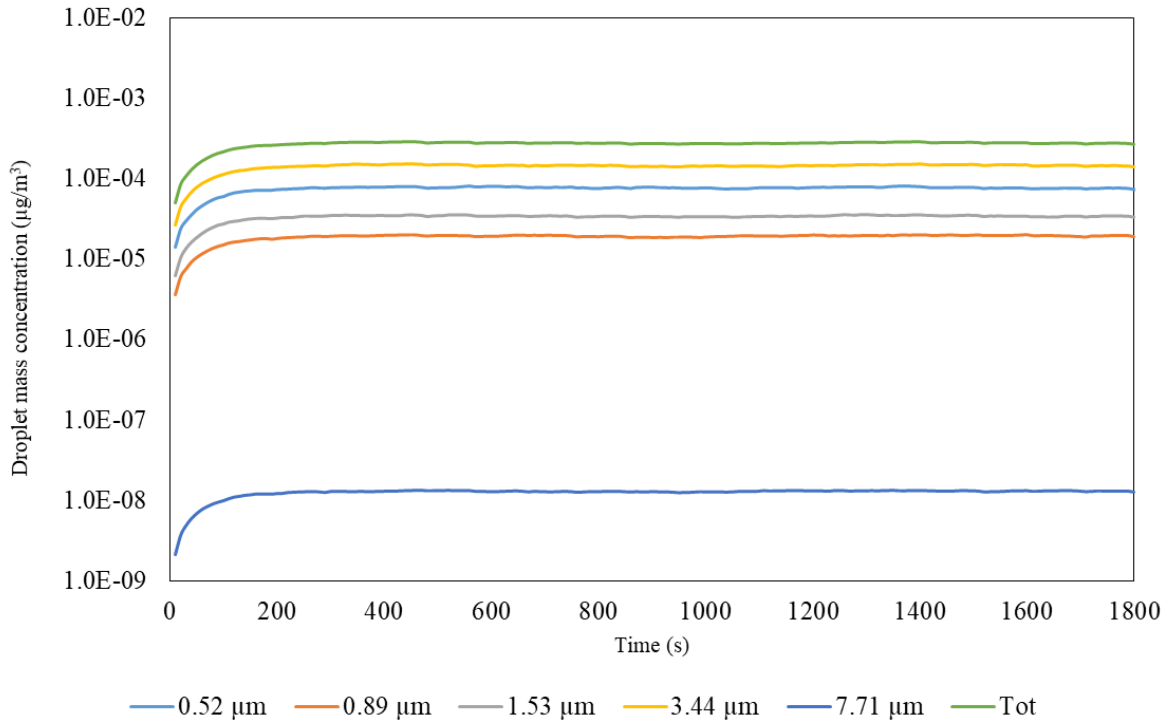


**Figure 5**. Time series of droplet mass concentration inside the domain D1 for different droplet diameters and for all the droplets (Tot).

The results of the simulations carried out in the domain D2 in order to establish a correlation between the droplet mass concentration and distribution and the air exchange rates is reported in the next Figures. Figure 6 shows the streamlines of the flow field inside the D2 domain for AER 1 and AER 7 at t = 900 s: as can be seen, for both the AER values and in relation to the air vents geometry there is a general pattern showing air that flows in two main directions: (i) along the vertical wall of the domain (bus windows), from top to bottom, and (ii) from the central top side to the central bottom side of the domain. This main flow structure leads to the definition of a high-turbulence zone in correspondence of the passenger seat that, together with the air flow generated from the personal air vents, tend to disperse, and transport the emitted droplets.

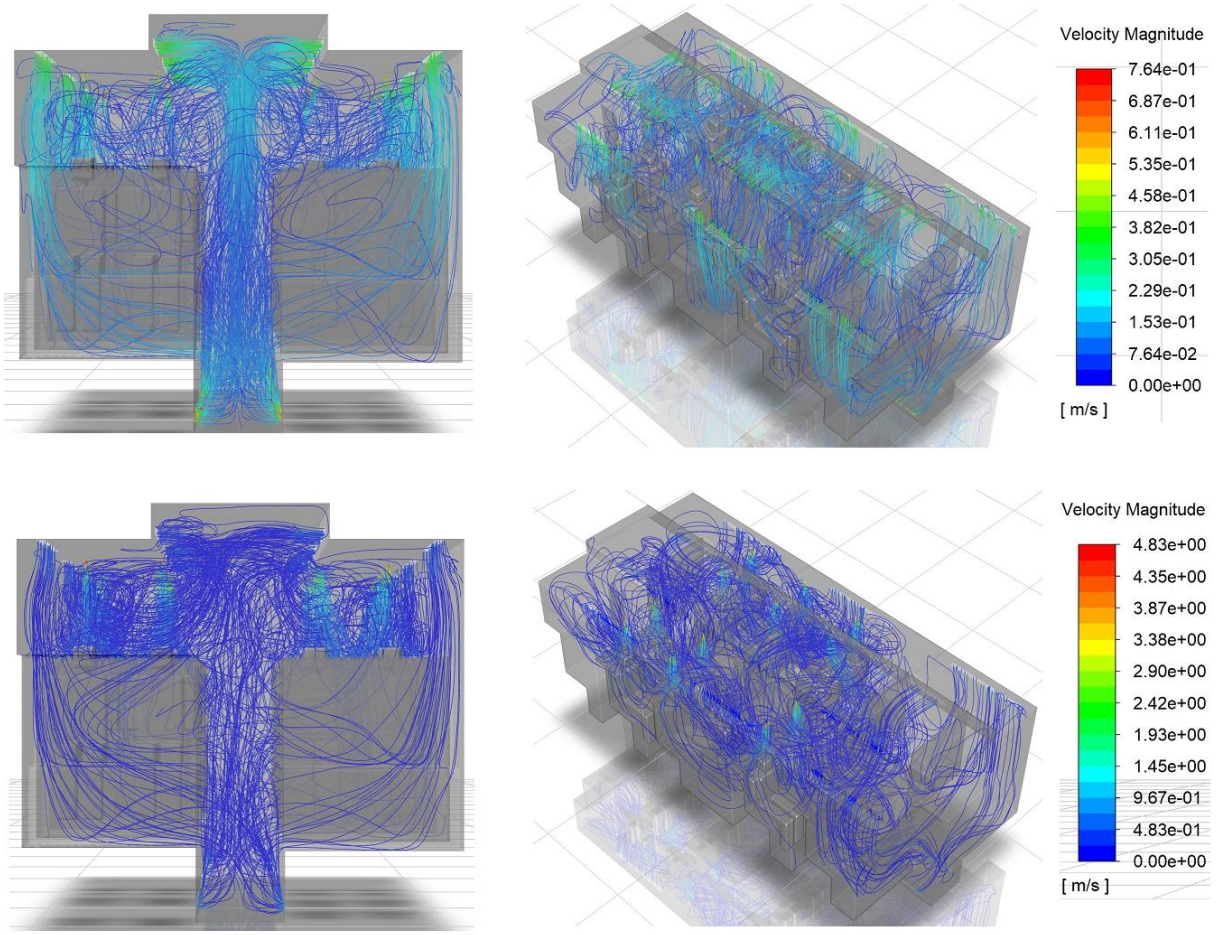


**Figure 6**. Streamlines of the flow structure in the domain D2 at time t=900 s: for AER 1 (top panel) and for AER 7 (bottom panel).

In Figure 7 the droplet distribution patterns inside the D2 domain are reported for the different AER values at t = 900 s. As can be seen, the droplets tend to be more dispersed inside the domain as the AER increase. It can also be observed that even though different droplet sizes were considered, the distribution at t = 900 s is characterized by a quite uniform mixing of droplets with different sizes since the dynamics is only slightly influenced by a small difference of droplet diameters.
Figure 8 reports the time series of droplet mass concentration inside the D2 domain, for different droplet diameters and for different AER values in the time interval 0 – 900 s. The patterns shown in this figure is similar to those showed in Figure 5, with concentration values that become constant after less than 100 s for AER 1, AER 3 and AER 7, while a small fluctuation in droplet mass concentration can be observed between 100 to 200 s for the case of AER 5, for all the droplet diameters. Even in this case the time series result the same for all the considered droplet sizes.

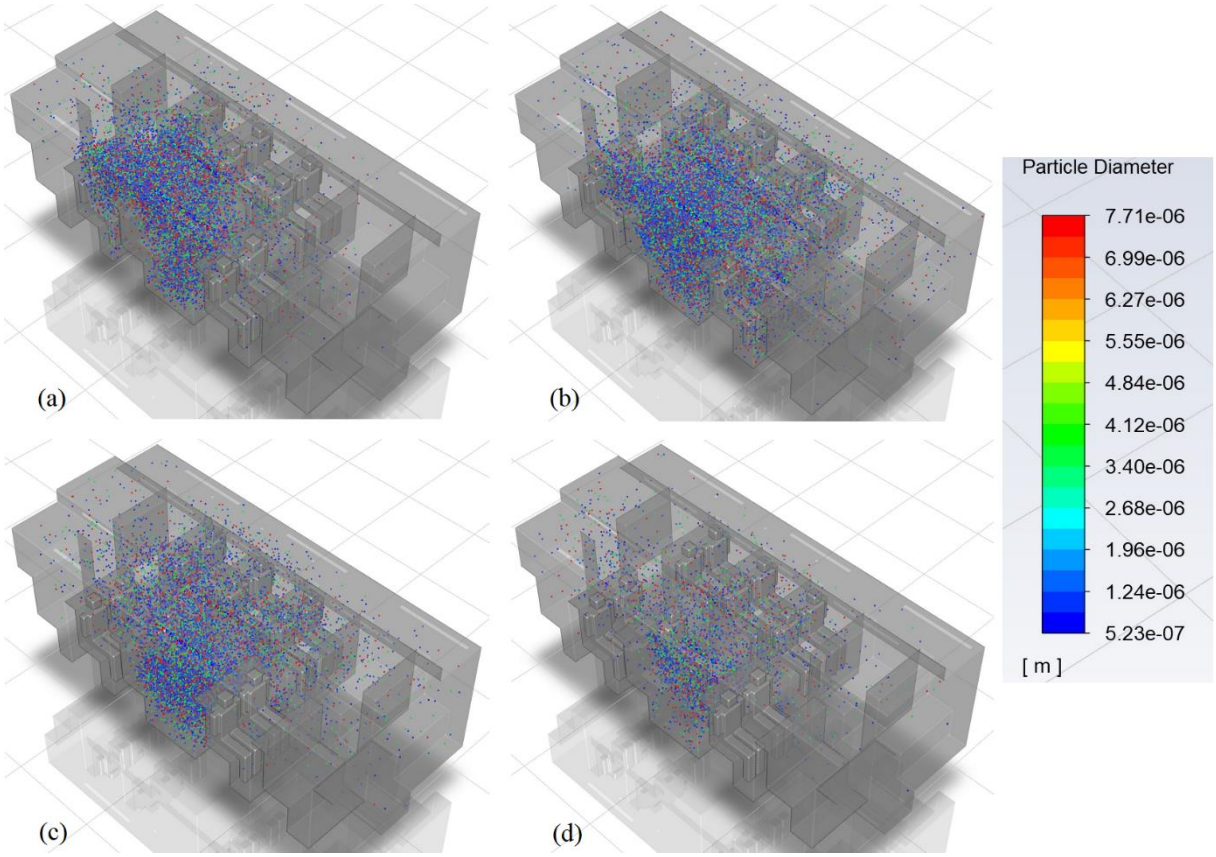


**Figure 7**. Droplet distributions inside the D2 domain for the different AER values at time t=900 s: AER 1 (a); AER 3 (b); AER 5 (c); AER 7 (d).

The results showed in Figure 8 are summarized in Table 5. Here the droplet mass concentration is evaluated as a mean value of concentration inside the domain between 300 – 900 s of simulation for all the droplet diameters and AER values. In the last line of the table, a total mass concentration value is reported as a sum of the concentration for all the droplet sizes.

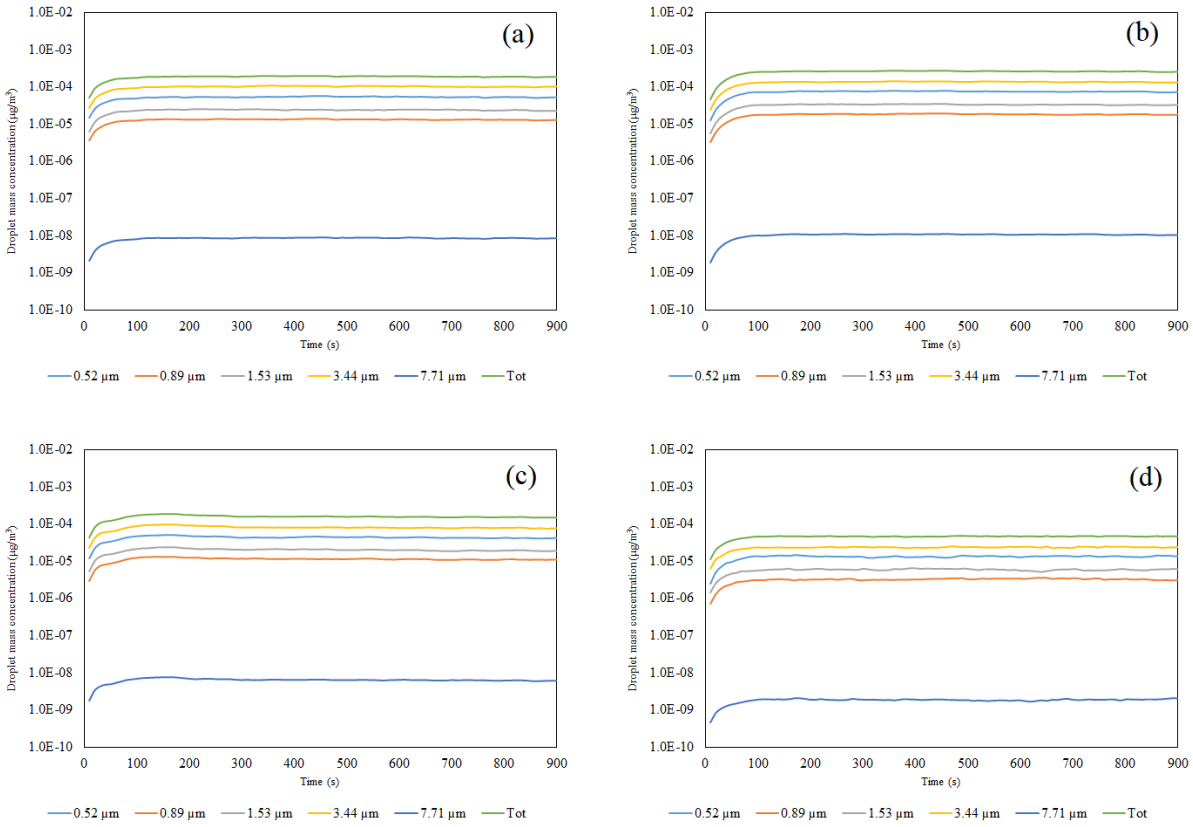


**Figure 8**. Time series of the droplet mass concentration inside the D2 domain for the different droplet diameters and for different AER values: AER 1 (a); AER 3 (b); AER 5 (c); AER 7 (d).

From the data reported in Table 5, it can be observed that as a general behavior there is a first increase of droplet mass concentration between AER 1 and AER 3, whit a maximum increase of about 38 % for the droplets of 0.89 µm in diameter and a total concentration that increases of about 35 %, and a subsequent continuous reduction of droplet concentration as the AER increases from 3 to 7. Looking at the differences from AER 1 to AER 7, there is a reduction in the total mass concentration of 75.4 %, with a maximum value of 78.1 % for droplets of 7.71 µm in diameter. This can be explained referring to the dynamic of the biggest droplets, characterized to be more affected by the gravity and with higher inertia, with the consequence to be more susceptible to deposit on the surfaces (domain walls). As a general remark, looking at Table 5 there is an increasing percentage of mass droplet reduction with the increasing of droplet size.

**Table 5**. Droplet mass concentration in the domain D2 reported as a main value between 300 s and 900 s for each considered value of air exchange rate and for the different droplet diameters. The last line of table reports the total mass concentration for all the droplet sizes.

| **Droplet diameter** | **Mean droplet mass concentration in the domain ($\mu g/m^3$, $t = 300 - 900$ s)** | | | |
|---|---|---|---|---|
| **(µm)** | **AER 1** | **AER 3** | **AER 5** | **AER 7** |
| 0.52 | 5.30E-05 | 7.30E-05 | 4.37E-05 | 1.31E-05 |
| 0.89 | 1.33E-05 | 1.83E-05 | 1.11E-05 | 3.33E-06 |
| 1.53 | 2.37E-05 | 3.24E-05 | 1.95E-05 | 5.90E-06 |
| 3.44 | 1.02E-04 | 1.36E-04 | 8.01E-05 | 2.43E-05 |
| 7.71 | 8.63E-09 | 1.10E-08 | 6.39E-09 | 1.89E-09 |
| **TOT** | **1.92E-04** | **2.60E-04** | **1.54E-04** | **4.67E-05** |

## 4. Conclusions

In this paper a set of CFD simulations were carried out in order to evaluate the influence of the ventilation strategy on the dispersion of respiratory droplets emitted inside a coach bus. Full 3D and time-dependent simulations were carried out using a DPM approach in order to evaluate the discrete phase (droplet) trajectory and a Standard k-ε turbulence model. A first domain consisting of the whole coach bus was considered in order to establish the main droplet dispersion patterns while a second one, consisting in a section of the bus, was realized in order to simulate different personal air exchange rates and analyze the influence of the personal ventilation on the droplet dispersion.

The simulation of the whole bus showed that the droplets tend to concentrate close to the emitter and that the concentration tends to become constant after a time period of 200 s for all the considered droplet sizes. By implementing the personal ventilation, it was observed that with the increase of the personal AER value, a reduction of the droplet mass concentration inside the domain can be achieved, with a maximum reduction of about 75 % passing from personal AER 1 to 7.

The results of the present paper show the importance of properly design the ventilation system inside a coach bus, and in particular referring to the personal air exchange rate, which if correctly designed can lead to a significant reduction of droplet concentration exposure and as a consequence a reduction of the risk of infection from airborne diseases.

## References

1. Organization, W.H., *Modes of transmission of virus causing COVID-19: implications for IPC precaution recommendations: scientific brief, 29 March 2020*. 2020, World Health Organization.
2. Ai, Z.T. and A.K. Melikov, *Airborne spread of expiratory droplet nuclei between the occupants of indoor environments: A review.* Indoor air, 2018. **28**(4): p. 500-524.
3. Lednicky, J.A., et al., *Viable SARS-CoV-2 in the air of a hospital room with COVID-19 patients.* International Journal of Infectious Diseases, 2020. **100**: p. 476-482.
4. Vuorinen, V., et al., *Modelling aerosol transport and virus exposure with numerical simulations in relation to SARS-CoV-2 transmission by inhalation indoors.* Safety Science, 2020. **130**: p. 104866.
5. Chattopadhyay, K., M. Isac, and R.I.L. Guthrie, *Considerations in using the discrete phase model (DPM).* steel research international, 2011. **82**(11): p. 1287-1289.
6. Feng, Y., et al., *Influence of wind and relative humidity on the social distancing effectiveness to prevent COVID-19 airborne transmission: A numerical study.* Journal of aerosol science, 2020. **147**: p. 105585.
7. Johnson, G., et al., *Modality of human expired aerosol size distributions.* Journal of Aerosol Science, 2011. **42**(12): p. 839-851.
8. Morawska, L., et al., *Size distribution and sites of origin of droplets expelled from the human respiratory tract during expiratory activities.* Journal of aerosol science, 2009. **40**(3): p. 256-269.
9. Cortellessa, G., et al., *Close proximity risk assessment for SARS-CoV-2 infection.* Science of The Total Environment, 2021. **794**: p. 148749.
10. Pirouz, B., et al., *CFD Investigation of Vehicle's Ventilation Systems and Analysis of ACH in Typical Airplanes, Cars, and Buses.* Sustainability, 2021. **13**(12): p. 6799.